



## Effects of Amplitude, Maximal Lyapunov Exponent, and Kaplan–Yorke Dimension of Dynamical Oscillators on Master Stability Function

Mohadeseh Shafiei Kafraj and Fahimeh Nazarimehr

*Department of Biomedical Engineering,  
Amirkabir University of Technology (Tehran Polytechnic), Iran*

Dibakar Ghosh

*Physics and Applied Mathematics Unit, Indian Statistical Institute,  
203 B. T. Road, Kolkata 700108, India*

Karthikeyan Rajagopal

*Centre for Nonlinear Systems,  
Chennai Institute of Technology, Chennai, India*

Sajad Jafari\*

*Department of Biomedical Engineering,  
Amirkabir University of Technology (Tehran Polytechnic), Iran*

*Health Technology Research Institute,  
Amirkabir University of Technology (Tehran Polytechnic), Iran  
sajadjafari@aut.ac.ir*

J. C. Sprott

*Department of Physics, University of Wisconsin – Madison,  
Madison, WI 53706, USA*

Received July 21, 2021; Revised November 8, 2021

Obtaining the master stability function is a well-known approach to study the synchronization in networks of chaotic oscillators. This method considers a normalized coupling parameter which allows for a separation of network topology and local dynamics of the nodes. The present study aims to understand how the dynamics of oscillators affect the master stability function. In order to examine the effect of various characteristics of oscillators, a flexible oscillator with adjustable amplitude, Lyapunov exponent, and Kaplan–Yorke dimension is used. Not surprisingly, it is demonstrated that the amplitude of the oscillations has no substantial effect on the master stability function, i.e. the coupling strength needed for the complete synchronization is not changed. However, the flexible oscillators with larger maximal Lyapunov exponent synchronize with larger coupling strength. Interestingly, it is shown that there is no linear connection between the Kaplan–Yorke dimension and coupling strength needed for complete synchronization.

*Keywords:* Synchronization; master stability function; chaos.

---

\*Author for correspondence

## 1. Introduction

Synchronization is an important collective behavior in networks of dynamical systems. This phenomenon has been observed in a wide range of complex networks, including networks of connected biological [Schöll, 2020], technological [Chowdhury & Khalil, 2021], and physical systems [Zhang & Strogatz, 2021]. For instance, in the brain as a complex network, synchronization is an integral feature of its dynamics at different scales of the nervous system, from neural activity to the entire brain [Traub et al., 2004; De Stefano et al., 2019; Wang et al., 2020]. In the literature, several studies have been done on synchronization [Dai et al., 2020; Chowdhury et al., 2019; Wang et al., 2019]. Researchers have examined the effect of different factors on synchronization, including coupling strength, time delays, and noise [Santos et al., 2019; Shi & Lu, 2009; Sun et al., 2015].

The synchronizability of a given network is first dependent on the network structure that describes the interaction between oscillators. Second, it is dependent on the local dynamics of oscillators [Lodi et al., 2020; Xi et al., 2020]. Master Stability Function (MSF) can determine the necessary and sufficient conditions for a network to reach a synchronized state [Pecora & Carroll, 1998]. MSF analyzes the synchronization independent of network topology, no matter how complex it is. In particular, the MSF is a maximal Lyapunov exponent of a set of variational equations. In variational equations, the dynamics of oscillators, type of couplings, and a normalized coupling parameter  $K$  are considered. Normalizing coupling parameter makes the analysis independent of the topology. Several works have studied the synchronization of single and multilayer networks with regular, small-world, and random typologies [Della Rossa & DeLellis, 2020; Barahona & Pecora, 2002; Della Rossa et al., 2020]. In a network of coupled oscillators, the necessary condition for synchronization is negative MSF for an interval of normalizing control parameter  $K$  [Pecora & Carroll, 1998]. Authors in [Huang et al., 2009] have introduced a general scheme to classify the behavior of MSFs in terms of crossing zero value into  $\Gamma_0, \Gamma_1, \dots, \Gamma_n$ . In this classification,  $\Gamma_m$  indicates that the MSF possesses  $m$  finite cross points. There are some research works that have focussed on MSF. To study a network with stochastic inner dynamics, an upgraded MSF was suggested [Della Rossa & DeLellis, 2020]. This method

concluded that if noise diffuses evenly in the network, it could benefit synchronization. Zero-lag and cluster synchrony of delay-coupled dynamical oscillators using the master stability approach was discussed in [Ladenbauer et al., 2013]. In [Berner et al., 2021], the MSF was used for various adaptive networks. MSF can also be developed for hypergraphs [Mulas et al., 2020]. MSF for various delay distributions and network structures was discussed in [Kyrychko et al., 2014]. In [Sun et al., 2009], a generalized MSF for a network of oscillators with small but arbitrary parametric changes was studied.

The present study seeks to address the question of “How amplitude, Maximal Lyapunov Exponent (MLE), and Kaplan–Yorke dimension ( $D_{KY}$ ) of chaotic oscillators impact the synchronization?” With this aim, the synchronization of two coupled flexible chaotic oscillators is studied. The term “flexible” means that the amplitude, MLE, and  $D_{KY}$  of the oscillator are controllable by proper control parameters [Chen et al., 2018; Munmuangsaen et al., 2015]. While it is predictable that the amplitude of oscillations does not affect their synchronizability and the MLE has a linear relation with the MSF, we are aware of no work in the literature discussing the effect of  $D_{KY}$  on the MSF. The paper is organized into four sections. In Sec. 2, we briefly provide the mathematics of the flexible chaotic system and MSF formulation. Section 3 examines how the amplitude, MLE, and  $D_{KY}$  of oscillators affect the MSF. Finally, in Sec. 4, the conclusion gives a summary and critique of the findings.

## 2. MSF for a Flexible Chaotic System Under $x - x$ Coupling Scheme

In the following, the formula of the flexible chaotic system and its corresponding MSF under  $x - x$  coupling scheme are presented.

### 2.1. System dynamics

The flexible system is defined as follows [Chen et al., 2018],

$$\begin{aligned} \dot{x} &= k_2 y, \\ \dot{y} &= k_2 \left( -x + \frac{yz}{k_1} \right), \\ \dot{z} &= k_2 (ak_1 - |y| - bz). \end{aligned} \quad (1)$$

This system was based on a previously analyzed system with an adjustable attractor dimension [Munmuangsaen *et al.*, 2015; Sprott, 2020] which is known as Buncha system. System (1) was proposed to have adjustable amplitude, MLE, and  $D_{KY}$  [Chen *et al.*, 2018]. The oscillator shows chaotic dynamics in  $a = 5$ ,  $b = 0.5$ ,  $k_1 = 1$  and  $k_2 = 1$  and initial conditions  $[6, 10, -2]$ . In the equations of the system,  $k_1$ ,  $k_2$ , and  $b$  are parameters that control the amplitude of oscillations, MLE, and  $D_{KY}$ , respectively [Chen *et al.*, 2018].

## 2.2. Master stability function

For a system described by  $\frac{dX_i}{dt} = F(X_i)$ ,  $i = 1, 2, \dots, N$ , where  $X_i$  is a  $m$ -dimensional vector of variables for the  $i$ th oscillator and  $F(X_i)$  defines the velocity field, a general form of the identical network is described by

$$\frac{dX_i}{dt} = F(X_i) - \varepsilon \sum_{j=1}^N G_{ij} H(X_j), \quad (2)$$

where  $N$  is the number of coupled oscillators, and  $\varepsilon$  is the strength of the global coupling. Here,  $G : R^N \rightarrow R^N$  is the coupling matrix satisfying

$$\frac{d\xi_k}{dt} = \left[ \begin{array}{cc} 0 & k_2 \\ -k_1 & \frac{k_2}{k_1} z \\ 0 & -k_2 \text{sign}(y) \end{array} \right] - K \left[ \begin{array}{ccc} 1 & 0 & 0 \\ 0 & 0 & 0 \\ 0 & 0 & 0 \end{array} \right] \xi_k. \quad (5)$$

It should be noted that for  $y$  values near zero,  $-0.005 < y < 0.005$ , the approximation  $\text{sign}(y) \approx \tanh(\omega y)$  with  $\omega = 500$  is considered.

## 3. Results

In a given network, synchronization can be affected by its topology (matrix  $G$ ), and coupling variables (matrix  $H$ ). Using the MSF method, the influence of network topology is considered as  $K_k = \varepsilon \mu_k$  ( $k \geq 2$ ); that is a multiplication of global coupling strength with corresponding eigenvalues of  $G$ . Once MSF is calculated based on the normalized parameter  $K$ , it can be applied to any network topology. To determine the synchronizable regions of coupling strength, all  $K_k$ s must be located in the region for which  $MSF < 0$ . The MSF for different coupling schemes is shown in Fig. 1. In the following,

$\sum_{j=1}^N G_{ij} = 0$ , and  $H : R^m \rightarrow R^m$  is the coupling function that determines which variables are coupled. Considering the synchronous state of the network  $\frac{ds}{dt} = F(s)$  with  $s = X_i$  for  $i = 1, 2, \dots, N$ , the block diagonally decoupled form of variational equation is as follows,

$$\frac{d\xi_k}{dt} = [DF(s) - KDH(s)]\xi_k. \quad (3)$$

$DF$  and  $DH$  are the Jacobian functions of  $F(s) : R^m \rightarrow R^m$ , and  $H(s) : R^m \rightarrow R^m$ .  $K$  is a normalized coupling parameter.  $K_k = \varepsilon \mu_k$  ( $k \geq 2$ ) is a specific set of  $K$  with  $\mu_k$  being a nonzero eigenvalue of the matrix  $G : R^N \rightarrow R^N$ , and  $0 = \mu_1 < \mu_2 \leq \mu_3 \leq \dots \leq \mu_N$  [Pecora & Carroll, 1998; Huang *et al.*, 2009]. Consequently, the MSF is defined as the MLE of Eq. (3). When oscillators are coupled via  $x$  variable, the Jacobian function of  $H(s)$  becomes,

$$DH = E = \begin{pmatrix} 1 & 0 & 0 \\ 0 & 0 & 0 \\ 0 & 0 & 0 \end{pmatrix}. \quad (4)$$

So the simplified form of Eq. (3) for the given system [Eq. (1)] is

all simulations are done using 5000 cycles of the system with a time-step of 0.01. The ODEs are approximated using the fourth-order Runge-Kutta method. The network's elements are coupled only through one variable, i.e. only one element of matrix  $DH$  is equal to one. So, each panel belongs to a different type of coupling. For instance, the notation  $x \rightarrow y$  determines that couplings are from the  $x$  variable of one oscillator to the  $y$  variable of its connected neighbors. Seeking intervals with negative MSF shows us that only through the  $x \rightarrow x$ ,  $y \rightarrow y$ , and  $z \rightarrow z$  coupling schemes, the network can be synchronized; otherwise, there is no possibility to reach the synchronized state. Besides network topology and coupling type, individual oscillators play a crucial role in synchronizing the network. The relevance between the synchronization of the

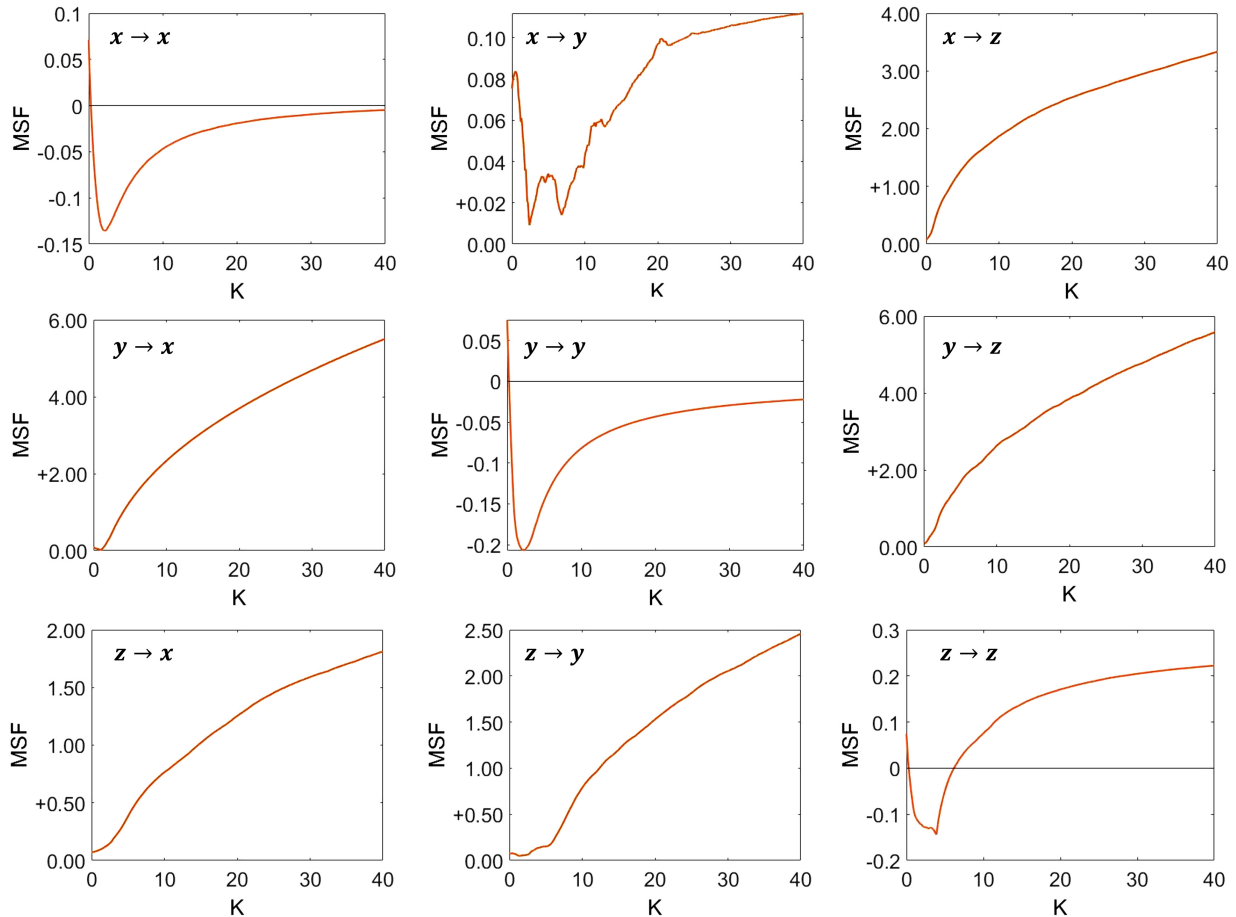


Fig. 1. MSFs of System (1) based on normalized parameter  $K$  for different coupling schemes. In each panel, the coupling types are specified by the name of involving variables in the coupling, e.g. the notation  $x \rightarrow y$  determines that couplings are from the  $x$  variable of one oscillator to the  $y$  variable of its connected neighbor. The system variables are set to  $a = 5$ ,  $b = 0.5$ ,  $k_1 = 1$ , and  $k_2 = 1$ .

network and the amplitude, MLE, and  $D_{KY}$  of the oscillator is discussed in the following subsections.

### 3.1. Amplitude

It is important to understand how the amplitude of oscillations impacts synchronization. In the following, it is considered that oscillators in

the network are coupled through  $x$  variable. The flexible chaotic system, Eq. (1), has an adjustable amplitude. Changing  $k_1$  results in change to the amplitude of the dynamics. Figure 2(a) shows how the amplitude of oscillations changes with parameter  $k_1$ . In this figure, the horizontal axis shows the amplitude control parameter, and the vertical axis shows the amplitude of the attractors. The amplitude is measured by

$$A = \sqrt{(X_{\max} - X_{\min})^2 + (Y_{\max} - Y_{\min})^2 + (Z_{\max} - Z_{\min})^2}. \tag{6}$$

$X_{\max}$ ,  $Y_{\max}$  and  $Z_{\max}$  are the maximum, and  $X_{\min}$ ,  $Y_{\min}$  and  $Z_{\min}$  are the minimum of oscillations in the settled attractor for the corresponding variables. As  $k_1$  increases, the attractor of the system expands. Figure 2(b) represents how MSF is changing by altering the parameters  $k_1$  and  $K$ . In this figure, the vertical axis is the normalized coupling parameter

$K$  in Eq. (3), and the horizontal axis is  $k_1$ . The color bar represents the value of MSF at each point  $(k_1, K)$ . It changes from positive to negative values. Positive values of MSF correspond to regions of  $(k_1, K)$  where the network cannot be synchronized. However, the negative values of MSF correspond to

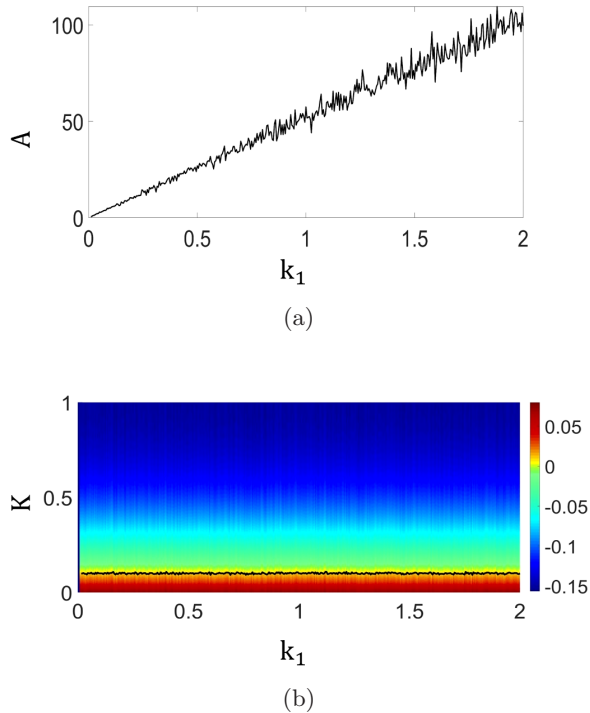


Fig. 2. The association between MSF and  $k_1$ , the parameter that changes the amplitude of the oscillations, for  $a = 5$ ,  $b = 0.5$ , and  $k_2 = 1$ . (a) The amplitude of oscillations by changing parameter  $k_1$ . (b) MSF values indicated by color bar for different values of  $k_1$ , and normalized coupling parameter  $K$ . The result shows that the zero-cross point of MSF, the black curve, does not change by changing parameter  $k_1$ , i.e. MSF is independent of the amplitude of oscillations.

the regions of  $(k_1, K)$  that the network potentially can be synchronized. The black curve is the first zero point of MSF in the direction of  $K$ . Results show that for the different amplitudes of oscillation, the black curve is approximately constant. It means that the zero-cross point of MSF, which defines the required coupling strength for synchronization, remains the same. Subsequently, changes in amplitude make the synchronization neither difficult nor easy.

### 3.2. Maximal Lyapunov exponent

Maximal Lyapunov exponent is an important feature of dynamical oscillators. A definition of deterministic chaos is relevant to positive MLE in the Lyapunov spectrum. For Eq. (1), the MLE is adjustable by parameter  $k_2$ . Figure 3(a) shows the dependence of the Lyapunov exponents (indicated by three different colors) on the parameter  $k_2$ . Figure 3(b) shows the relation between MLE and MSF. The value of MSF related to each point  $(k_2, K)$  is depicted by a color bar. The black curve

is the first zero point of MSF in the direction of  $K$ . This curve shows a boundary range of  $k_2$  and  $K$  that the network potentially can or cannot be fully synchronized. The results show two conclusions. First, the zero-cross point of MSF increases as the MLE increases. It means that as the MLE of the oscillators increases, more coupling strength is needed to synchronize the network. Second, the shape of MSF contours is not changing by varying  $k_2$ . The zero-cross point of MSF is linearly dependent on  $k_2$ .

### 3.3. Kaplan–Yorke dimension

Besides MLE, other Lyapunov exponents are also informative for a dynamic system. Specifically for a chaotic system,  $D_{KY}$  is obtained from its Lyapunov spectrum as,

$$D_{KY} = d + \sum_{i=1}^d \frac{\lambda_i}{\lambda_{d+1}}, \quad (7)$$

where  $d$  is the largest number of descending Lyapunov exponents whose summation is non-negative.

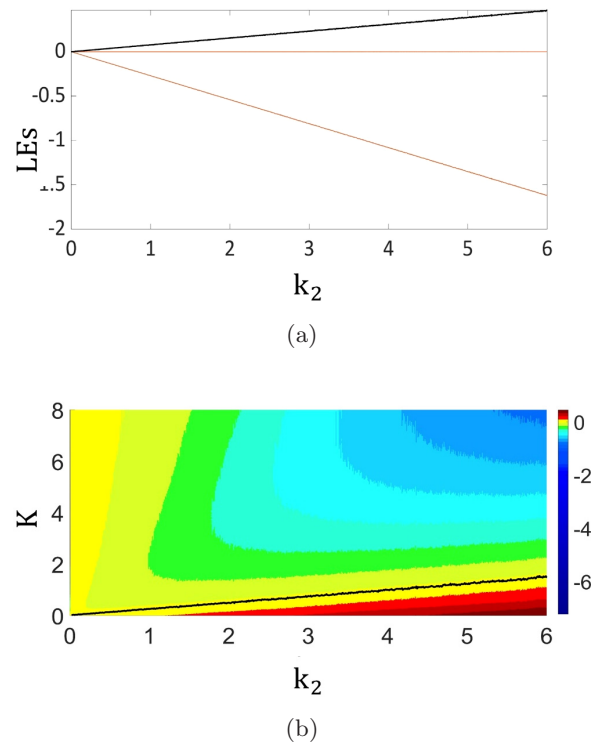


Fig. 3. The association between MSF and  $k_2$ , the parameter that changes MLE of the oscillator, for  $a = 5$ ,  $b = 0.5$ , and  $k_1 = 1$ . (a) The LEs versus parameter  $k_2$  and (b) MSF values indicated by colors based on MLE control parameter  $k_2$ , and normalized coupling parameter  $K$ . The result shows that the zero-cross point, the black curve, increases as the MLE increases. So, the more the oscillators are chaotic, more coupling strength is needed to synchronize their network.



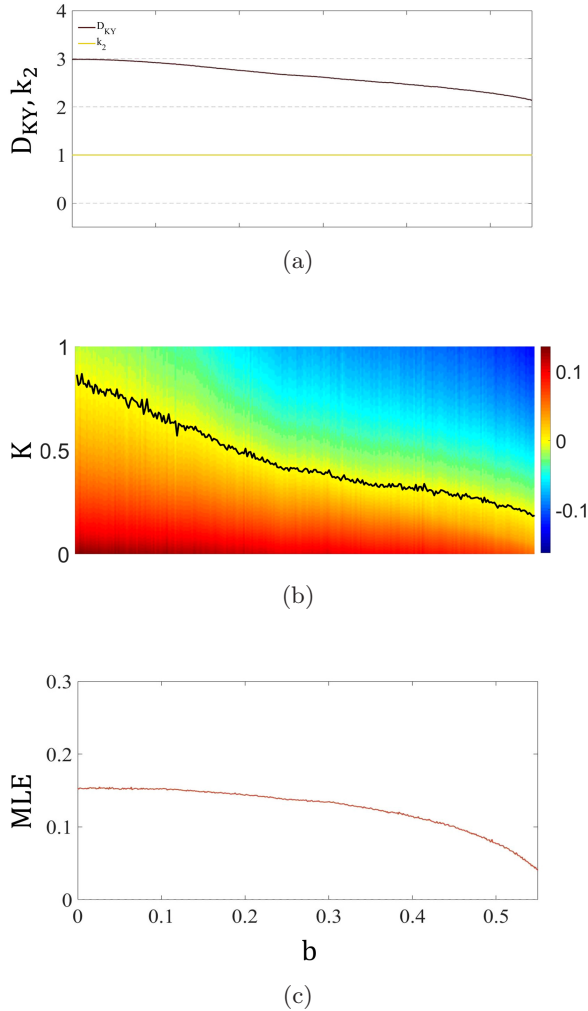


Fig. 4. The association between MSF and  $D_{KY}$  control parameter for a constant  $k_2 = 1$ . (a) The  $D_{KY}$ , and  $k_2$  values versus parameter  $b$ , (b) MSF values indicated by color bar based on  $D_{KY}$  control parameter  $b$ , and normalized coupling parameter  $K$  and (c) MLE values versus parameter  $b$ . Here,  $a$  and  $k_1$  parameters are set to  $a = 5$ , and  $k_1 = 1$ .

In System (1)  $D_{KY}$  can be controlled using parameter  $b$ . In Fig. 4, the impact of  $D_{KY}$  on MSF is studied. In this case, as shown in Fig. 4(a), only the parameter  $b$  varies and  $k_2 = 1$ . It shows that as  $b$  increases, the  $D_{KY}$  changes from  $D_{KY} = 3$  to almost 2. So the dynamics change from conservative chaos to dissipative chaos. From Fig. 4(b), it can be discussed that synchronization is strongly associated with the dimension of the oscillations. In this figure, the horizontal axis belongs to control parameter  $b$ , and the vertical axis is normalized parameter  $K$ . Values of  $D_{KY}$  associated with  $(b, K)$  points are indicated by the color bar. The black curve that is the first zero point of MSF in the direction of  $K$ , shows the necessary condition

to reach a synchronized state. Therefore, it could be concluded that the smaller  $D_{KY}$  results in a smaller zero-cross point, which corresponds to smaller coupling strength required for synchronization. However unlike the previous case, this does not happen in a linear way. The important point here is that as the  $D_{KY}$  changes, the MLE changes, too [Fig. 4(c)]. So it is necessary to find a way to examine the effect of  $D_{KY}$  independently. As seen in Sec. 3.2, the MLE has a linear relation with  $k_2$ . To keep the MLE constant on a value named MLE(desired), an adaptive parameter  $k_2$  named  $k_2(\text{desired})$  can be

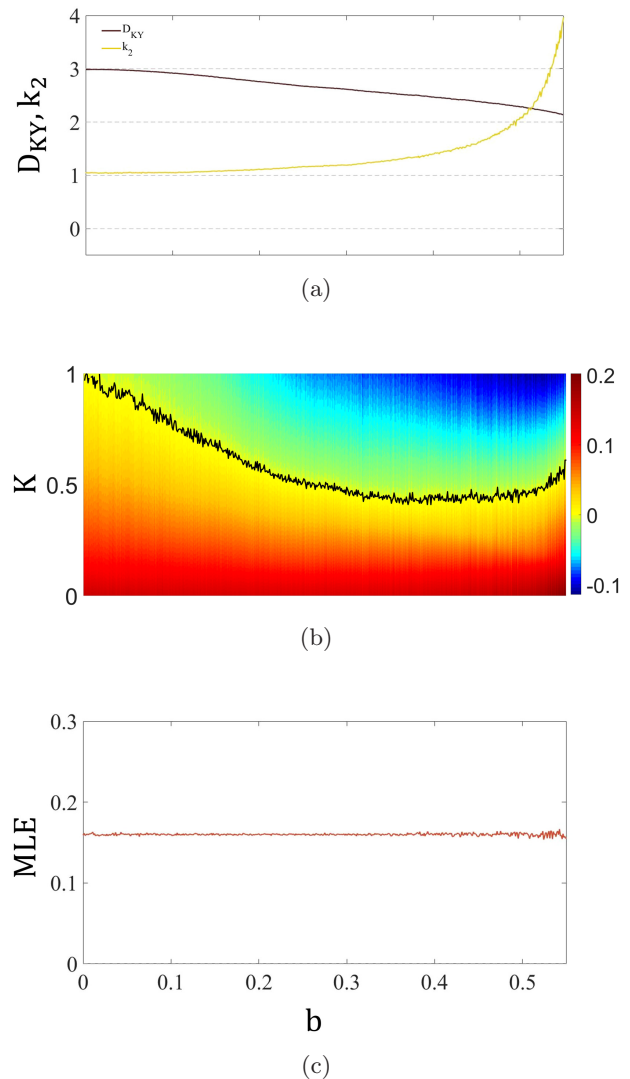


Fig. 5. The association between MSF and  $D_{KY}$  control parameter for updated  $k_2$  values. (a) The  $D_{KY}$ , and  $k_2$  values versus parameter  $b$ , (b) MSF values indicated by color bar based on  $D_{KY}$  control parameter  $b$ , and normalized coupling parameter  $K$  with adaptive  $k_2$  and (c) MLE values versus parameter  $b$ . Here,  $a$  and  $k_1$  parameters are set to  $a = 5$ , and  $k_1 = 1$ .

used according to the following formula,

$$\frac{\text{MLE}(\text{desired})}{\text{MLE}} = \frac{k_2(\text{desired})}{k_2}. \quad (8)$$

Considering the result presented in Fig. 4 for  $k_2 = 1$  and setting the desired value of MLE to  $\text{MLE}(\text{desired}) = 0.16$ , it is obtained that

$$k_2(\text{desired}) = \frac{0.16}{\text{MLE}}. \quad (9)$$

This calculation results in a vector of  $k_2$  values by changing  $b$ . In the next step, at each point, both  $k_2$  values and  $b$  values change. For each parameter  $b$ , a corresponding value of  $k_2$  is determined. Then the MSF in each  $(k_2, b)$  point is calculated. Figure 5 shows that by selecting adaptive  $k_2$  values, the MLE is kept approximately constant. So, in this condition, any change in the MSF is associated with  $D_{KY}$ , independent of MLE. It is found out that as  $D_{KY}$  decreases, the first zero point of MSF in the direction of  $K$  has a decreasing nonlinear trend. However, by decreasing  $D_{KY}$  more than a threshold, the first zero point of MSF in the direction of  $K$  increases.

#### 4. Conclusion

This study set out to determine the impact of the dynamics of oscillators on synchronization. To this aim, the MSFs associated with a flexible chaotic system were examined. The results indicated that for  $x \rightarrow x$ ,  $y \rightarrow y$ , and  $z \rightarrow z$  coupling schemes, a network of flexible chaotic oscillators could be synchronized through type  $\Gamma_1$ . Otherwise, it could not be synchronized. Considering the  $x \rightarrow x$  coupling type for the network, it was shown that the amplitude of oscillations does not influence synchronization. Then the effect of MLE on the MSF was investigated. It was shown that as the MLE of the chaotic oscillator increased by increasing parameter  $k_2$ , the zero-cross point moved to a larger value. So, more coupling strength was needed to reach the synchronized state. Further, as the Kaplan–Yorke dimension became smaller by increasing parameter  $b$ , the zero-cross point became smaller. However, by decreasing  $D_{KY}$  more than a threshold, the zero point of MSF increased.

#### Acknowledgment

This work is funded by the Center for Nonlinear Systems, Chennai Institute of Technology, India, via funding number CIT/CNS/2021/RD/007.

#### Conflict of Interest

The authors declare no conflict of interest.

#### References

- Barahona, M. & Pecora, L. M. [2002] “Synchronization in small-world systems,” *Phys. Rev. Lett.* **89**, 054101.
- Berner, R., Vock, S., Schöll, E. & Yanchuk, S. [2021] “Desynchronization transitions in adaptive networks,” *Phys. Rev. Lett.* **126**, 028301.
- Chen, H., Bayani, A., Akgul, A., Jafari, M.-A., Pham, V.-T., Wang, X. & Jafari, S. [2018] “A flexible chaotic system with adjustable amplitude, largest Lyapunov exponent, and local Kaplan–Yorke dimension and its usage in engineering applications,” *Nonlin. Dyn.* **92**, 1791–1800.
- Chowdhury, S. N., Majhi, S., Ozer, M., Ghosh, D. & Perc, M. [2019] “Synchronization to extreme events in moving agents,” *New J. Phys.* **21**, 073048.
- Chowdhury, D. & Khalil, H. K. [2021] “Practical synchronization in networks of nonlinear heterogeneous agents with application to power systems,” *IEEE Trans. Autom. Contr.* **66**, 184–198.
- Dai, X., Li, X., Gutiérrez, R., Guo, H., Jia, D., Perc, M., Manshour, P., Wang, Z. & Boccaletti, S. [2020] “Explosive synchronization in populations of cooperative and competitive oscillators,” *Chaos Solit. Fract.* **132**, 109589.
- Della Rossa, F. & DeLellis, P. [2020] “Stochastic master stability function for noisy complex networks,” *Phys. Rev. E* **101**, 052211.
- Della Rossa, F., Pecora, L., Blaha, K., Shirin, A., Klickstein, I. & Sorrentino, F. [2020] “Symmetries and cluster synchronization in multilayer networks,” *Nature Commun.* **11**, 3179.
- De Stefano, L. A., Schmitt, L. M., White, S. P., Mosconi, M. W., Sweeney, J. A. & Ethridge, L. E. [2019] “Developmental effects on auditory neural oscillatory synchronization abnormalities in autism spectrum disorder,” *Front. Integr. Neurosci.* **13**, 34.
- Huang, L., Chen, Q., Lai, Y.-C. & Pecora, L. M. [2009] “Generic behavior of master-stability functions in coupled nonlinear dynamical systems,” *Phys. Rev. E* **80**, 036204.
- Kyrychko, Y. N., Blyuss, K. B. & Schöll, E. [2014] “Synchronization of networks of oscillators with distributed delay coupling,” *Chaos* **24**, 043117.
- Ladenbauer, J., Lehnert, J., Rankoohi, H., Dahms, T., Schöll, E. & Obermayer, K. [2013] “Adaptation controls synchrony and cluster states of coupled threshold-model neurons,” *Phys. Rev. E* **88**, 042713.
- Lodi, M., Della Rossa, F., Sorrentino, F. & Storaice, M. [2020] “Analyzing synchronized clusters in neuron networks,” *Scient. Rep.* **10**, 16336.

- Mulas, R., Kuehn, C. & Jost, J. [2020] “Coupled dynamics on hypergraphs: Master stability of steady states and synchronization,” *Phys. Rev. E* **101**, 062313.
- Munmuangsaen, B., Sprott, J. C., Thio, W. J.-C., Buscarino, A. & Fortuna, L. [2015] “A simple chaotic flow with a continuously adjustable attractor dimension,” *Int. J. Bifurcation and Chaos* **25**, 1530036-1–12.
- Pecora, L. M. & Carroll, T. L. [1998] “Master stability functions for synchronized coupled systems,” *Phys. Rev. Lett.* **80**, 2109–2112.
- Santos, M. S., Protachevich, P. R., Iarosz, K. C., Caldas, I. L., Viana, R. L., Borges, F. S., Ren, H.-P., Szezech Jr, J. D., Batista, A. M. & Grebogi, C. [2019] “Spike-burst chimera states in an adaptive exponential integrate-and-fire neuronal network,” *Chaos* **29**, 043106.
- Schöll, E. [2020] “Chimeras in physics and biology: Synchronization and desynchronization of rhythms,” *Nova Acta Leopoldina* **425**, 67–95.
- Shi, X. & Lu, Q. [2009] “Burst synchronization of electrically and chemically coupled map-based neurons,” *Physica A* **388**, 2410–2419.
- Sprott, J. [2020] “Variants of the Nosé–Hoover oscillator,” *The Europ. Phys. J. Special Topics* **229**, 963–971.
- Sun, J., Bollt, E. M. & Nishikawa, T. [2009] “Master stability functions for coupled nearly identical dynamical systems,” *Europhys. Lett.* **85**, 60011.
- Sun, X.-J., Han, F., Wiercigroch, M. & Shi, X. [2015] “Effects of time-periodic intercoupling strength on burst synchronization of a clustered neuronal network,” *Int. J. Nonlin. Mech.* **70**, 119–125.
- Traub, R. D., Bibbig, A., LeBeau, F. E., Buhl, E. H. & Whittington, M. A. [2004] “Cellular mechanisms of neuronal population oscillations in the hippocampus in vitro,” *Ann. Rev. Neurosci.* **27**, 247–278.
- Wang, Y., Lu, J., Liang, J., Cao, J. & Perc, M. [2019] “Pinning synchronization of nonlinear coupled Lur’e networks under hybrid impulses,” *IEEE Trans. Circuits Syst.-II: Express Briefs* **66**, 432–436.
- Wang, Y., Shi, X., Cheng, B. & Chen, J. [2020] “Synchronization and rhythm transition in a complex neuronal network,” *IEEE Access* **8**, 102436–102448.
- Xi, X., Panahi, S., Pham, V.-T., Wang, Z., Jafari, S. & Hussain, I. [2020] “Optimum topology and coupling strength for synchronization,” *Appl. Math. Comput.* **379**, 125226.
- Zhang, Y. & Strogatz, S. H. [2021] “Designing temporal networks that synchronize under resource constraints,” *Nature Commun.* **12**, 3273.